JOURNAL OF THERMOPHYSICS AND HEAT TRANSFER
Vol. 7, No. 1, Jan.–March 1993

Longitudinal Heat Dispersion in Porous Beds with Real-Gas Flow

M. Sözen* and K. Vafai†
Ohio State University, Columbus, Ohio 43210

The forced convective flow of a slightly superheated vapor through a packed bed is analyzed numerically for low-to-moderate pressure range by implementing real-gas and ideal-gas models. The porous bed was taken to be composed of uniformly sized, randomly packed spherical particles. The flow of the gas through the packed bed was limited to the range of applicability of the Ergun-Forchheimer relation. The significance of longitudinal thermal dispersion was examined by alternately implementing and omitting this aspect which was incorporated in the effective thermal conductivity of the vapor phase. The use of a real-gas model at elevated pressures was found to be an important aspect for accurate results. The longitudinal thermal dispersion effects were found to have minor significance at high Reynolds numbers. The use of separate energy equations for the solid and vapor phases was observed to be justified by the studies performed.

Nomenclature

a_{sv} = specific surface area of the bed particles, m^2/m^3
c_p = specific heat at constant pressure, J/kg-K
d_p = particle diameter, m
F = geometric factor defined in Eq. (8)
h_{sv} = fluid-to-particle heat transfer coefficient, W/m^2-K
K = permeability, m^2
k = thermal conductivity, W/m-K
L = length of the packed bed, m
P = pressure, N/m^2
Pr = Prandtl number, $\mu c_p/k$
R = gas constant for Refrigerant-11, J/kg-K
Re_p = particle Reynolds number, $u\rho d_p/\mu$
T = temperature, K
t = time, s
u = velocity component in x direction, m/s
Z = compressibility factor
ε = porosity
μ = absolute viscosity, kg/m-s
ρ = density, kg/m^3
$\langle\ \rangle$ = local volume average of a quantity

Subscripts
ax = longitudinal
d = dispersion
eff = effective
s = solid
seff = effective property for solid
v = vapor
veff = effective property for vapor
0 = initial

Superscripts
s = solid
v = vapor
0 = stagnant

Received Oct. 14, 1991; revision received March 1, 1992; accepted for publication March 5, 1992.

*Post Doctoral Research Associate, Department of Mechanical Engineering.
†Professor of Mechanical Engineering, Department of Mechanical Engineering. Member AIAA.

I. Introduction

ACCURATE simulation of the heat and mass transport phenomena in packed beds has been an important aspect in the process design of packed bed reactors and other applications such as energy storage systems. In achieving this, all aspects of flow and transport phenomena have to be accounted for. In this regard, the flow in porous media brings the consideration of thermal dispersion into attention. In a porous medium, a fluid flows in tortuous paths recirculating at the back of the particles. This phenomenon of fluid mixing (recirculation or dispersion) results in both a pressure drop across the medium and a net increase in energy transport. The effect of this thermal dispersion has been formulated by establishing empirical correlations for the effective thermal conductivity which accounts for the thermal dispersion effects.

A literature survey reveals that extensive attention has been given to studies on the determination of the radial and axial effective thermal conductivities in cylindrical packed beds, the former receiving the majority of earlier attention. Investigations by Yagi and Kunii,[1,2] Yagi et al.,[3] and Gunn and De Souza,[4] report experiments on measurement of these quantities, whereas, investigations by Hunt and Tien[5] provide some insight on the physics of the dispersion phenomenon. In establishing the effective thermal conductivity accounting for the thermal dispersion effects, the same methodology of splitting it into stagnant and dispersion components has been the basis in different investigations. This method assumes that the effective thermal conductivity, axial (longitudinal) or radial, consists of the effective thermal conductivity at stagnant state plus that when the fluid moves through the packed bed. In the correlations established in this way for the axial and radial directions the stagnant component is expressed in terms of the phase fractions and the individual thermal conductivities of the phases, whereas, the dispersion component is simply expressed as a factor of $(Re_p Pr)$.

It should be mentioned that to our knowledge the investigations performed to date for establishing these correlations experimentally, assume that the local temperature difference between the solid and fluid phases is negligible, i.e., there is local thermal equilibrium (LTE) between the two phases. Therefore, the established effective thermal conductivity refers to the packed bed system with the working fluid. The LTE certainly is not a necessary assumption, and actually becomes a poor assumption in forced convective flows. Since LTE assumption results in a single energy equation, the effective thermal conductivity in the aforementioned investi-

gations is associated with the temperature gradient of the system of packed bed with the working fluid. It is, however, possible to use separate energy equations for the solid phase and the working fluid and still make use of the existing correlations that were established by using the assumption of LTE in a systematic way. The fact that the solid phase is fixed within the packed bed, and that dispersion part of the effective thermal conductivity can be attributed to the fluid phase, forms the basis of this approach. Accomplishing the demonstration of this point is one of the major objectives of the present work and will be elaborated in the following section. The effect of considering the axial thermal dispersion effects will be explored for flows with relatively high speed compared to Darcy flows.

Another objective of the present investigation is to qualitatively show the difference between utilization of real- and ideal-gas models for a typical working fluid in a slightly superheated state. At such a state the vapor is close to a saturation state where the real-gas effects would be expected to be more pronounced than in the case of highly superheated states. These effects are expected to be magnified at elevated pressures. The authors[6,7] have analyzed the transport phenomena in compressible and condensing flows through packed beds by modeling the working fluid as an ideal gas. By the rigorous models established in these investigations, the qualitative behavior of the field variables was clearly demonstrated. Certain characteristics of compressible flows through porous media and factors affecting the two-dimensionality of the problem and the validity of the LTE assumption were also reported. The present study concentrates on the working fluid being modeled as a real gas; exploring the qualitative differences between ideal- and real-gas models and the effect of axial (or longitudinal) thermal dispersion on the bulk energy transport in forced convective flows in packed beds.

II. Mathematical Formulation

The physical problem considered is the one-dimensional forced convective flow of slightly superheated Refrigerant-11(R-11) through a packed bed of finite length, namely 20 cm. It should be noted that the results presented here represent the behavior of most real gases. The packed bed is assumed to be formed by spherical particles of uniform diameter. Figure 1 depicts the schematic diagram of the problem. Initially, working fluid at uniform pressure and in local thermal equilibrium with the bed particles is assumed to be present within the packed bed. Superheated vapor 50 K above the initial bed temperature and at a higher pressure is allowed to flow through the bed. Since the packed bed can be cylindrical or a rectangular one, the term "longitudinal" will be used instead of "axial."

The problem has been formulated by the authors[6,8] using the "local volume averaging" technique with implementation of an ideal-gas model for the working fluid. Here, an extension is made by modeling the working fluid as a real gas. This is accomplished by the use of Z, in the equation of state. The volume-averaged governing equations are as follows:

$$\frac{\partial}{\partial t}(\varepsilon\langle\rho_v\rangle^v) + \frac{\partial}{\partial x}(\langle\rho_v\rangle^v\langle u_v\rangle) = 0 \tag{1}$$

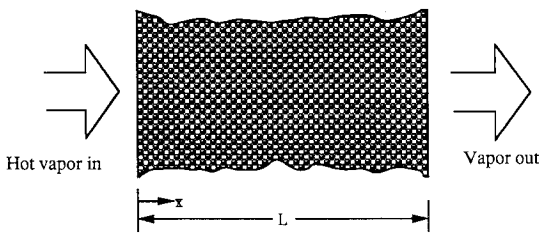

Fig. 1 Schematic diagram of the problem.

$$\frac{\partial\langle P_v\rangle^v}{\partial x} = -\frac{\langle\rho_v\rangle^v F\varepsilon}{K_v^{1/2}}\langle u\rangle^2 - \frac{\mu_v}{K_v}\langle u_v\rangle \tag{2}$$

$$\varepsilon\langle\rho_v\rangle^v c_{p_v}\frac{\partial\langle T_v\rangle^v}{\partial t} + c_{p_v}\langle\rho_v\rangle^v\langle u_v\rangle\frac{\partial\langle T_v\rangle^v}{\partial x} = \frac{\partial}{\partial x}\left(k_{\text{veff}}\frac{\partial\langle T_v\rangle^v}{\partial x}\right) + h_{sv}a_{sv}(\langle T_s\rangle^s - \langle T_v\rangle^v) \tag{3}$$

$$(1-\varepsilon)\rho_s c_{p_s}\frac{\partial\langle T_s\rangle^s}{\partial t} = \frac{\partial}{\partial x}\left(k_{\text{seff}}\frac{\partial\langle T_s\rangle^s}{\partial x}\right) - h_{sv}a_{sv}(\langle T_s\rangle^s - \langle T_v\rangle^v) \tag{4}$$

$$\langle P_v\rangle^v = \langle\rho_v\rangle^v ZR\langle T_v\rangle^v \tag{5}$$

where Z is the compressibility factor for Refrigerant-11 and has been correlated for the temperature and pressure ranges of the present study, namely 290–420 K and 90–750 kPa respectively, in terms of the reduced temperature T_r and reduced pressure P_r as

$$Z(T_r, P_r) = 1.19465947 - 0.82727862T_r + 0.70035598T_r^2 - 0.68865164P_r + 0.54981776P_r^2 \tag{6}$$

Equations (1–5) represent the vapor phase continuity equation, vapor phase momentum equation, vapor phase energy equation, solid phase energy equation, and vapor phase equation of state, respectively. The five field variables computed from these equations are $\langle\rho_v\rangle^v$, $\langle u_v\rangle$, $\langle T_v\rangle^v$, $\langle T_s\rangle^s$, and $\langle P_v\rangle^v$, respectively. It should be noted that our results represent the main qualitative features for flow of gases through a packed bed.

Based on the Ergun-Forchheimer relation, the permeability of the packed bed K_v and the geometric function F in Eq. (2) can be obtained from investigations reported by Ergun[9] and Vafai[10] in the form

$$K_v = [\varepsilon^3 d_p^2/150(1-\varepsilon)^2] \tag{7}$$

$$F = (1.75/\sqrt{150}\varepsilon^{3/2}) \tag{8}$$

whereas, the specific surface area of the particles in the packed bed can be modeled as[11]

$$a_{sv} = [6(1-\varepsilon)/d_p] \tag{9}$$

Determination of the fluid-to-particle heat transfer coefficient h_{sv} has received extensive attention by many researchers, and depending on the range of particle Reynolds number and Prandtl number of the fluid of application as well as the shape and size of the particles of the bed, specific correlations can be found in the literature. Some of the most up-to-date literature reviews on h_{sv} have been reported by Wakao et al.[12,13] Based on the average of a wide range of experimental findings, the corrected correlation for the Nusselt number Nu, considering thermal dispersion, is given by[13]

$$Nu = 2 + 1.1Pr^{1/3}Re_p^{0.6} \tag{10}$$

and has been used in the present investigation. For stagnant condition, the effective conductivities can be expressed as

$$k_{\text{veff}}^0 = \varepsilon k_v \qquad k_{\text{seff}}^0 = (1-\varepsilon)k_s \tag{11}$$

For the case with fluid motion, and hence, dispersion, we first consider the single-phase energy equation approach, i.e., LTE assumption. For this case, the effective longitudinal thermal

conductivity is

$$(k_{\text{eff}})_{ax} = k^0_{\text{eff}} + k_d \tag{12}$$

where k^0_{eff} is the stagnant conductivity and k_d is the dispersion conductivity. Here, the dispersion phenomenon has been modeled as a diffusive phenomenon as has been done by previous investigators.[5] Although the correlations for k_d reported by different investigators show considerable variation, it is widely accepted that the contribution of fluid mixing to the effective longitudinal thermal conductivity is a factor of $d_p u \rho_v c_{p_v}$, and for a wide range of Re_p for the evaluation of $(k_{\text{eff}})_{ax}$ the following relation is recommended[13]

$$[(k_{\text{eff}})_{ax}/k_v] = (k^0_{\text{eff}}/k_v) + 0.5(Pr_v)(Re_p) \tag{13}$$

where, from Eq. (11) $k^0_{\text{eff}} = \varepsilon k_v + (1 - \varepsilon)k_s$ and a comparison of Eq. (13) with Eq. (12) reveals the fact that the difference between $(k_{\text{eff}})_{ax}$ and k^0_{eff} is equal to $k_d = 0.5(Pr_v)(Re_p)k_v$, which represents the contribution of fluid mixing (dispersion) to the transfer of heat in the longitudinal direction. Therefore, although a relation of the type given in Eq. (12) is based on the single-phase approach, it is very reasonable to associate k_d to the temperature gradient of the fluid phase, and k^0_{veff} and k^0_{seff} (which constitute k^0_{eff}) to the temperature gradient of the fluid phase and solid phase, respectively. Thus, for cases with fluid motion in the packed bed, the effective thermal conductivities with longitudinal thermal dispersion effects have been modeled as

$$\begin{aligned} k_{\text{veff}} &= \varepsilon k_v + 0.5(Pr_v)(Re_p)k_v \\ k_{\text{seff}} &= (1 - \varepsilon)k_s \end{aligned} \tag{14}$$

For completeness of the mathematical model, one needs to specify the porosity of the packed bed and the particle diameter. The latter is taken to be 2 mm for practical purposes, whereas, the former is taken to be 0.39 based on the average value determined by experimental findings.[14] Also, the variation of the thermophysical properties with temperature was neglected and the following values were used in the numerical simulations.

Refrigerant-11 (vapor phase)	1% Carbon-steel (solid phase)
$c_p = 608$ J/kg-K	$c_p = 473$ J/kg-K
$k = 0.00955$ W/m-K	$k = 43$ W/m-K
$\mu = 11.95 \times 10^{-6}$ kg/m-s	$\rho = 7800$ kg/m^3
$R = 60.51827$ J/kg-K	

The initial conditions for the problem were

$$\begin{aligned} P_v(x, t = 0) &= P_0 \\ T_v(x, t = 0) &= T_s(x, t = 0) = T_0 \\ u_v(x, t = 0) &= 0 \end{aligned} \tag{15}$$

whereas, the value of ρ_v was computed from Eq. (5). The boundary conditions used were

$$\begin{aligned} P_v(x = 0, t) &= P_{\text{vin}} \\ P_v(x = L, t) &= P_0 \\ T_v(x = 0, t) &= T_{\text{vin}} \end{aligned} \tag{16}$$

while again Eq. (5) yields the value of ρ_v for the inlet and exit of the packed bed.

III. Method of Solution

The intercoupled nature of Eqs. (1–5) does not allow for a closed-form analytical solution. Therefore, these equations were solved by using an explicit scheme finite-difference method. Euler forward-differencing was used in approximating the temporal derivative terms. Central differencing was employed in approximating the spatial derivative terms for the inner grid points, except in the convective terms of the vapor phase continuity and energy equations for which first order upwind differencing was implemented. Another exception was the use of forward-differencing in approximating the pressure gradient term in the vapor phase momentum equation. These provisions were made to insure the stability and accuracy of the numerical scheme. For the spatial derivative terms for the left and right boundary grid points, forward and backward differencing were respectively employed. Due to this, no boundary conditions were required for variable T_s since it could be directly computed from Eq. (4).

The solution was obtained by choosing a proper combination of grid size Δx, and time step Δt. Accuracy of the solution was improved by systematically decreasing Δx and choosing a Δt which yielded convergent solution. The solutions obtained by using 41 grid points were basically the same within 2% as those obtained by using 81 grid points. Therefore, case studies were carried out by using 41 grid points for CPU economy. For the ideal-gas model version of the numerical code used in the present work, two bench marks were reported by the authors[6] for two simplified cases of flow and energy transport in porous media. The solutions were in very good agreement with the analytical solutions for those simplified cases.

IV. Results and Discussions

As stated earlier, the present study concentrated on qualitatively showing the significance of longitudinal thermal dispersion effects on forced convective flows as well as the real-gas effects for a typical working fluid at low-to-moderate pressures. Since the thermal dispersion effects have been modeled as a function of Re_p and the Prandtl number of the working fluid, case studies were performed for a range of particle Reynolds numbers. Variation within the gaseous Prandtl numbers is small, and therefore, the results obtained in the present investigation will provide general qualitative features for the flow of gases through a porous bed. Different Reynolds numbers were obtained by applying different inlet pressures while keeping the initial pressure (i.e., the exit pressure) the same. In order to examine the real-gas effects we performed case studies at different pressure levels. Starting with a low 100 kPa for the initial pressure, cases with initial pressures of 200 and 700 kPa were also carried out. In order to make sure that R-11 was always in a superheated state, the initial and inlet vapor temperatures of 320 and 370 K were used respectively for the case with 200-kPa initial pressure, and 370 and 420 K for the case with 700 kPa initial pressure, i.e., 50-K difference was always maintained between the inlet and initial vapor temperatures. One final point that has been accomplished in the present study is the justification of the use of the two-energy equation model for accurate temperature simulation in the two phases.

It will help to first look at the variation of the field variables during a typical thermal charging process of the packed bed. For a detailed discussion the reader may refer to previous works[6,7] where results for ideal-gas flow without thermal dispersion effects were presented in detail. Figure 2 depicts the variation of the five field variables with time and space. These results are for the case with $P_0 = 100$ kPa, $T_0 = 300$ K, $T_{\text{vin}} = 350$ K and $P_{\text{vin}} = 112$ kPa which resulted in a nominal Re_p of 1570. The vapor density in this figure was nondimensionalized with respect to an average density value computed by using the averages of the inlet and initial temperatures and pressures of the working fluid. In a similar manner, the vapor velocity was nondimensionalized with respect to a nominal velocity value computed from Eq. (2) by using the average density and the overall applied pressure gradient. As may be seen from the figure, the difference between the solid and fluid phase temperatures can be quite significant even after the two become almost the same at the inlet of the packed bed. Therefore, use of separate energy equations for the solid and vapor phases becomes necessary for accurate solutions.

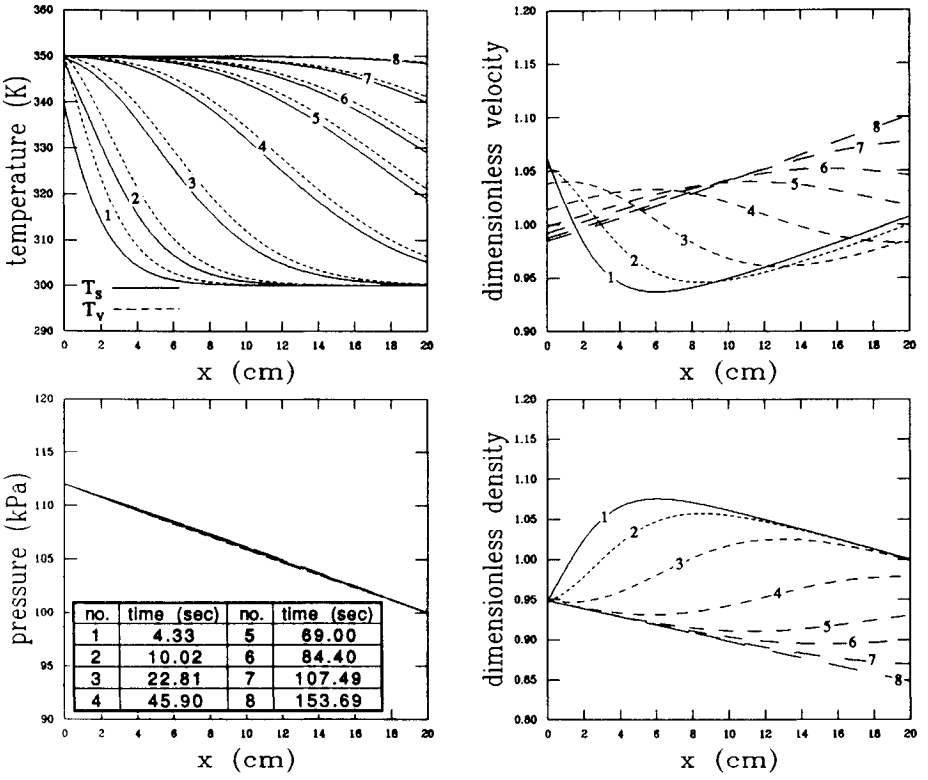

no.	time (sec)	no.	time (sec)
1	4.33	5	69.00
2	10.02	6	84.40
3	22.81	7	107.49
4	45.90	8	153.69

Fig. 2 Variation of different field variables during thermal charging of the packed bed.

Three different models were used in order to accomplish the objectives of this study. In the first of these models, model I, R-11 was modeled as a real gas and thermal dispersion effects were implemented [using Eq. (14)]. In model II, R-11 was modeled as an ideal gas [by using $Z = 1$ in Eq. (5)] and thermal dispersion effects were implemented as in model I. In model III, R-11 was modeled as a real gas but thermal dispersion effects were not implemented [Eq. (11) was used rather than Eq. (14)]. In order to perform systematic comparisons, the eighth grid point downstream of the packed bed inlet (i.e., 4 cm into the packed bed) was considered as the reference point.

The comparisons were performed as follows: for each nominal Re_p, the numerical code for model I was run until the time at which the temperature of the vapor phase at the reference point reached 25 K above the initial temperature. Subsequently, the numerical codes for models II and III were run for exactly the same amount of real time for the same initial and boundary conditions. The vapor temperatures obtained by the three models for the reference point were then compared. Taking the temperature obtained by model I as basis, comparisons with the values obtained by the other two models were made. These comparisons are depicted in Figs. 3 and 4 as relative differences. The relative difference between the temperature computed by model II or III and model I was found from

$$\text{difference} = \frac{|T_{\text{model I}} - T_{\text{model X}}|}{T_i(x = 0, t) - T_i(x, t = 0)} \cdot 100\% \quad (17)$$

where the denominator represents the difference between the initial and inlet vapor temperatures with respect to which the relative difference is computed, and numerically has the same value for all the cases regardless of the pressure level, and X stands for model II or III. Figure 3 gives the comparison between models I and III, and therefore, depicts the significance of the longitudinal thermal dispersion effects. Although a very clear trend of increase in dispersion effects with Reynolds number can be observed from this figure, the relative difference values in temperature show that these effects have a very minor influence. As a matter of fact, in previous

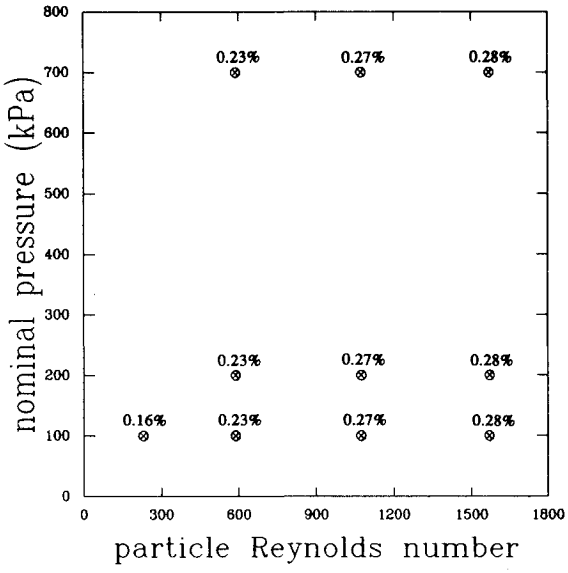

Fig. 3 Comparison of the results of model I vs model III.

investigations with incompressible working fluid, Vortmeyer[15] reported that only at Re_p of less than 50 would longitudinal dispersion effects cause any appreciable effects. Gunn and De Souza[4] also reported that thermal dispersion becomes dominant at Re_p of less than one.

Figure 4 shows a similar comparison between the solutions of models I and II. It should be noted that the particle Reynolds number is based on the nominal value for model I. Since the same temperature and pressure boundary conditions were used in each model, the nominal Re_p for model II were somewhat different from that of model I since a value of one is used for Z in the latter one, whereas, Z has a value of less than or equal to one in the former one. This explains the percent difference shown in Fig. 4. As the pressure level increases, the compressibility factor deviates more from the value of one (i.e., becomes smaller) and the use of an ideal-gas equation of state results in lower densities than what would

be predicted by a real-gas equation of state. Therefore, for the same pressure and temperature boundary and initial conditions the nominal Re_p for model II is smaller than that of model I, resulting in a smaller mass flow rate and smaller amount of thermal energy input to the packed bed. It is reasonable to observe that with model II it will take a longer time for the reference point to reach a given temperature than with model I, and this is the reason for the temperature of the reference point predicted by model II to be lower than that predicted by model I for any given real time. As the pressure level increases, the compressibility effects become more pronounced, resulting in a larger difference in the computed temperatures from these two models (as can be clearly seen in Fig. 4). The slight increase in the temperature difference as Re_p increases is due to the same reason, since larger Re_p is obtained by increasing the inlet pressure and subsequently increasing the average pressure at which the Z value is evaluated.

Finally, the difference between the solid and fluid phase temperatures was examined for each model separately. The qualitative and quantitative behavior observed in the findings of each of these models were practically the same. Therefore, the results are presented in Fig. 5 for model I only. The relative difference between the solid and vapor phase temperatures was computed by using Eq. (17) in which T_{ModelI} and T_{ModelN} were replaced by the vapor and solid phase temperatures at the reference point, respectively. As may be seen in this figure, the difference between the solid and fluid phase temperatures increases with Re_p. This is reasonable since as Re_p increases the flow speed increases and the thermal interaction time between the two phases decreases. The magnitude of the difference between the solid and fluid phase temperatures justifies the use of separate energy equations for these phases.

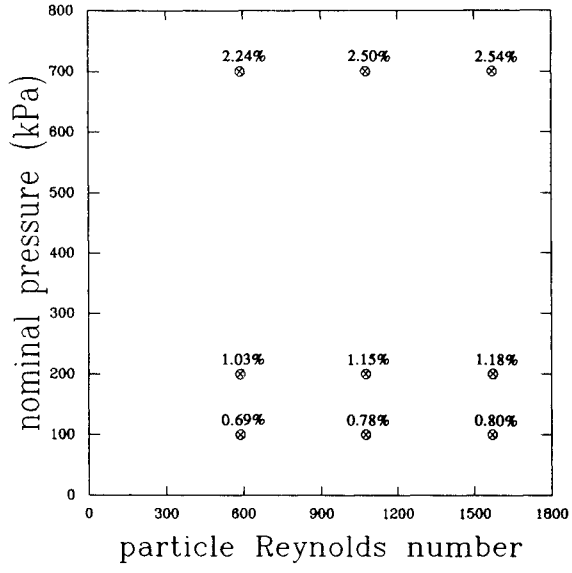

Fig. 4 Comparison of the results of model I vs model II.

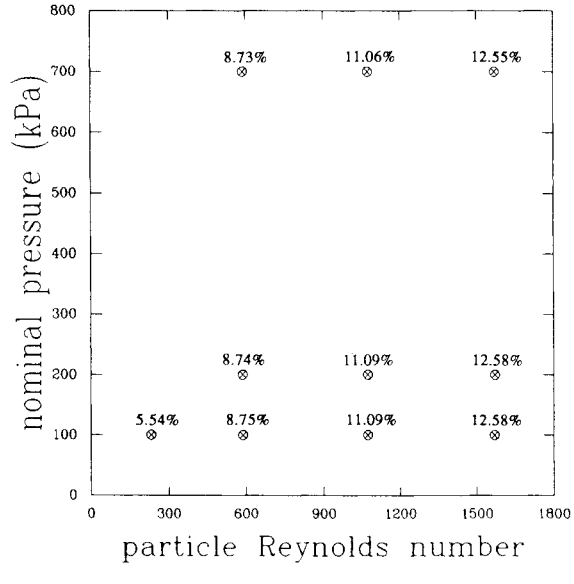

Fig. 5 Comparison of solid and vapor phase temperatures.

V. Conclusions

A mathematical model was developed for simulating energy and momentum transport in a real-gas flow through a packed bed, and a finite-difference method was used for solution. The analysis performed showed that the effects of longitudinal thermal dispersion were minor for high Reynolds number flows. As expected, compressibility effects were found to increase with the increase in the operating pressure, and from the investigation it can be concluded that for moderate-to-high pressures a real-gas model for the working fluid would increase the accuracy of the solution over an ideal-gas model. The results also showed that for forced convective flows the use of separate energy equations for the solid and vapor phases definitely increases the accuracy in simulating the temperature distribution and energy storage in the packed bed.

Acknowledgments

The support by the Aero Propulsion Laboratory of the USAF under Contract F33615-89-C-2949 and the grant by the Ohio Supercomputer Center is acknowledged and appreciated. The authors acknowledge W. Chang, J. E. Beam, and T. Mahefkey for their support and help on this project.

References

[1]Yagi, S., and Kunii, D., "Studies on Effective Thermal Conductivities in Packed Beds," *AIChE Journal*, Vol. 3, No. 3, 1957, pp. 373–381.

[2]Yagi, S., and Kunii, D., "Studies on Heat Transfer Near Wall Surface in Packed Beds," *AIChE Journal*, Vol. 61, No. 1, 1960, pp. 97–104.

[3]Yagi, S., Kunii, D., and Wakao, N., "Studies on Axial Effective Conductivities in Packed Beds," *AIChE Journal*, Vol. 6, No. 4, 1960, pp. 543–546.

[4]Gunn, D. J., and De Souza, J. F. C., "Heat Transfer and Axial Dispersion in Packed Beds," *Chem. Eng. Sci.*, Vol. 29, 1974, pp. 1363–1371.

[5]Hunt, M. L., and Tien, C. L., "Effects of Thermal Dispersion on Forced Convection in Fibrous Media," *International Journal of Heat and Mass Transfer*, Vol. 31, No. 2, 1988, pp. 301–309.

[6]Vafai, K., and Sözen, M., "Analysis of Energy and Momentum Transport for Fluid Flow Through a Porous Bed," *Journal of Heat Transfer*, Vol. 112, 1990, pp. 690–699.

[7]Sözen, M., and Vafai, K., "Analysis of the Non-Thermal Equilibrium Condensing Flow of a Gas Through a Packed Bed," *International Journal of Heat and Mass Transfer*, Vol. 33, 1990, pp. 1247–1261.

[8]Sözen, M., and Vafai, K., "Analysis of Oscillating Compressible Flow Through a Packed Bed," *International Journal of Heat and Fluid Flow*, Vol. 12, 1991, pp. 130–136.

[9]Ergun, S., "Fluid Flow Through Packed Columns," *Chem. Eng. Prog.*, Vol. 48, 1952, pp. 89–94.

[10]Vafai, K., "Convective Flow and Heat Transfer in Variable Porosity Media," *Journal of Fluid Mechanics*, Vol. 147, 1984, pp. 233–259.

[11]Dullien, F. A. L., *Porous Media Fluid Transport and Pore Structure*, Academic Press, New York, 1979.

[12]Wakao, N., Kaguei, S., and Funazkri, T., "Effect of Fluid Dispersion Coefficients on Particle-to-Fluid Heat Transfer Coefficients in Packed Beds," *Chem. Eng. Sci.*, Vol. 34, 1979, pp. 325–336.

[13]Wakao, N., and Kaguei, S., *Heat and Mass Transfer in Packed Beds*, Gordon & Breach, New York, 1982.

[14]Benanati, R. F., and Brosilow, C. B., "Void Fraction Distribution in Beds of Spheres," *AIChE Journal*, Vol. 8, No. 3, 1962, pp. 359–361.

[15]Vortmeyer, D., "Axial Heat Dispersion in Packed Beds," *Chem. Eng. Sci.*, Vol. 30, 1975, pp. 999–1001.